Supplementary information for the paper entitled "Attempt to distinguish electric signals of a dichotomous nature"

P. A. Varotsos,[1,*] N. V. Sarlis,[1] and E. S. Skordas[1]

[1] *Solid State Section, Physics Department, University of Athens, Panepistimiopolis, Zografos 157 84, Athens, Greece*

This supplementary information is organized as follows: Section I provides some additional information on the time-series analyzed, while Section II does so for the skewness, kurtosis and the non-Markovianity measure G. Section III and IV offer some background information on the Detrended Fluctuation Analysis (DFA) and the wavelet transform, respectively. Section V provides clarifications on some methods applied to the natural time domain, while Section VI describes the results expected for the application of DFA to a dichotomous Markovian time-series. Finally Section VII give additional information on the K-means clustering algorithm.

PACS numbers: 05.40.-a, 87.17.-d

I. THE TIME-SERIES ANALYZED

The RTS feature of signals mentioned in Fig.1 of the main text allows us to construct the time-series of subsequently high-level (T_h) and low-level (T_l) durations (dwell times) $\{T_{h,j}\}_{j=1}^{N_h}$, $\{T_{l,j}\}_{j=1}^{N_l}$, where N_h and N_l ($= N_h - 1$) are the total number of the high- and low-level states' durations, respectively. We clarify that the high-level states correspond to those having the largest deflections of the electric field amplitude with respect to the background level, low-level state. Table I presents the length of each time-series (sampling rate f_{exp} =1Hz), the number of transitions between the high and low levels $N_{tr} = N_l + N_h + 1$, and the average life-time $\langle T_h \rangle$ and $\langle T_l \rangle$ of the high and low level states, respectively, for the SES activities and "artificial" noises mentioned in Fig.1 of the main text.

II. THE NON-MARKOVIANITY MEASURE G. SKEWNESS AND KURTOSIS.

Here, we further investigate the non-Markovianity of SES and "artificial" noises and proceed to the calculation of the non-Markovian quantitative global measure G as defined in Ref.[1]. Following the recent illuminating study of Ref.[2], the definition of G can be summarized as follows. One of the properties of a Markov process is that it satisfies the Smoluchowski-Chapman-Kolmogorov (SCK) equation, and the deviation from this equation measures the degree of non-Markovianity:

$$D_{m,n}(t,\tau) = P(m,t|n,0) - \sum_{k=1}^{M} P(m,t|k,t-\tau)P(k,t-\tau|n,0)$$

where $k,m,n = 1,2,\ldots M$ number the electric field states (cf. in our case we have $M = 2$ different states labeled "high", $m = 1$, and "low", $m = 2$, respectively). The electric field belongs to the mth state when it lies in the interval $mdE < E < (m+1)dE, m = 0,\ldots,M-1$, $dE = (E_{max} - E_{min})/M$. The $P(m,t|n,s)$ is the field-field conditional probability that the electric field $E(t)$ is in the state number m, under the condition that at the earlier time $s < t$, $E(s)$ was in the state number n. The integral measure (mean square characteristics) of the non-Markovianity is[1, 2]

$$G = G(\tau,T) = \left[\frac{1}{T}\frac{1}{M^2}\sum_{m,n}^{M}\int_{\tau}^{\tau+T} D_{m,n}^2(t,\tau)dt\right]^{1/2} \quad (1)$$

where T is the range of the time t and τ is the shift in the SCK equation. As an example, for the cases K1 and n1, the calculation for $T = 100s$ yields $G_{max}(= sup_\tau G(\tau,T)) = 0.107 \pm 0.002$ and 0.135 ± 0.004, respectively. For computer-generated Markovian dichotomous series of comparable length, the corresponding $G-$values are smaller by one order of magnitude, which also suggests the non-Markovian character of the experimental data.

The non-Markovianity was also investigated by calculating the properties of the dwell-time distributions. The coefficients of skewness γ_1 and kurtosis β_2 are[3] $\gamma_1 = \mu_3/\sigma^3$ and $\beta_2 = \mu_4/\sigma^4$, where μ_n denotes the $n-$th central moment, i.e., $\mu_n = \sum_s (x_s - \mu)^n p_s$ of the randomly distributed data x_s with point probabilities p_s, respectively. These two coefficients γ_1 and β_2 are tabulated in Table II, along with σ^2/μ^2 for the series of the high (T_h) and low (T_l) level states' durations for all the SES activities and "artificial" noises. For a Markovian process (e.g. [4]) both T_h and T_l should follow exponential distributions, $p(\mathrm{T}) = \lambda \exp(-\lambda \mathrm{T})$, and in the ideal case of $f_{exp} \to \infty$ and $N_{tr} \to \infty$ the values $\sigma^2/\mu^2 = 1$, $\gamma_1 = 2$ and $\beta_2 = 9$ are expected. A Monte Carlo simulation(10^4 realizations) of exponentially distributed life-times having the same values of: (i) f_{exp}, (ii) number of events $N(=N_h$ or $N_l)$ and (iii) $\lambda(=1/\langle T_h \rangle$ or $1/\langle T_l \rangle)$ with the experimental ones, was performed for each SES activity and "artificial" noise. Comparing

*Electronic address: pvaro@otenet.gr

TABLE I: The length, the number of transitions N_{tr}, the average dwell time in the "high" $\langle T_h \rangle$ and the "low" $\langle T_l \rangle$ states for the time-series of SES activities and "artificial" noises mentioned in Fig.1 of the main text. The quantity $\langle T \rangle$, defined by $1/\langle T \rangle \equiv 1/\langle T_h \rangle + 1/\langle T_l \rangle$, is also shown.

Signal	Length (s)	N_{tr}	$\langle T_h \rangle$ (s)	$\langle T_l \rangle$ (s)	$\langle T \rangle$ (s)
K1	11899	626 ± 2	11.01 ± 0.03	25.37 ± 0.20	7.678 ± 0.018
K2	4160	276 ± 6	14.62 ± 0.11	14.62 ± 0.27	7.31 ± 0.07
A	4500	120 ± 12	24 ± 5	60 ± 10	17.1 ± 2.7
U	1750	173 ± 3	11.2 ± 1.2	9.2 ± 0.5	5.05 ± 0.29
n1	13000	438 ± 4	12.1 ± 0.5	43.5 ± 0.6	9.5 ± 0.3
n2	48000	2280 ±70	7.68 ± 0.24	31.9 ± 1.5	6.19 ± 0.16
n3	14999	568 ± 16	6.0 ± 1.0	33.1 ± 1.9	5.08 ± 0.07
n4	12610	660 ± 80	5.0 ± 0.6	29 ± 5	4.3 ± 0.4
n5	8100	810 ± 60	10.9 ± 2.5	10.2 ± 1.0	5.3 ± 0.6
n6	2650	84 ± 2	26.1 ± 0.5	33.2 ± 1.1	14.61 ± 0.26

the resulting values with those of Table II(see the relevant footnotes), we find that none of the time-series under discussion could be compatible with an exponential distribution and hence Markovian. The dwell-time distributions of the high-level states $\{T_{h,j}\}_{j=1}^{N_h}$ of the SES activities were also incompatible with the Gaussian distribution since the Kolmogorov-Smirnov test fails.

III. CONVENTIONAL AND MULTIFRACTAL DETRENDED FLUCTUATION ANALYSIS.

In the conventional DFA[5, 6], we first sum up the original time-series and determine the profile $y(i), i = 1, \ldots, N$. We then divide this profile of length N into $N/l(\equiv N_l)$ non overlapping fragments of l-observations. Next, we define the detrended process $y_{l,\nu}(\mathrm{m})$, in the $\nu-$th fragment, as the difference between the original value of the profile and the local (linear) trend. We then calculate the mean variance of the detrended process

$$F^2_{DFA}(l) = \frac{1}{N_l} \sum_{\nu=1}^{N_l} F^2(l,\nu), \tag{2}$$

where

$$F^2(l,\nu) = \frac{1}{l} \sum_{\mathrm{m}=1}^{l} y^2_{l,\nu}(\mathrm{m}) \tag{3}$$

The slope of the plot $\log[F_{DFA}(l)]$ versus $\log l$, leads to the value of the exponent α in the relation $F_{DFA}(l) \sim l^{\alpha}$. In our case, since the time-series is recorded with a frequency f_{exp}, we use the plot $\log(F_{DFA})$ versus $\log(\Delta t)$, because $\Delta t = l/f_{exp}$.

A generalization of the DFA to a multifractal method was first suggested in Ref.[7] and further elaborated in Ref.[8]. In the MF-DFA, the following additional two steps should be made[8]: First, we average over all segments to obtain the $q-$th order fluctuation function

$$F_q(l) \equiv \left\{ \frac{1}{N_l} \sum_{\nu=1}^{N_l} \left[F^2(l,\nu)\right]^{q/2} \right\}^{1/q}. \tag{4}$$

This is repeated for several scales l. Second, we analyze the log-log plots $F_q(l)$ versus l for each value of q. For long-range correlated series, $F_q(l)$ increases, for large values of l, as a power law:

$$F_q(l) \sim l^{h(q)}, \tag{5}$$

where the function $h(q)$ is called generalized Hurst exponent. For stationary time series, $h(2)$ is identical[8] to the well known Hurst exponent H,i.e.,

$$h(2) = H. \tag{6}$$

For monofractal time-series $h(q)$ is independent of q, while for multifractal series $h(q)$ depends on q.

A. Relation of MF-DFA to standard multifractal analysis

The scaling exponent $\tau(q)$ in the standard multifractal formalism is connected to the partition function $Z_q(l)$ through

$$Z_q(l) \sim l^{\tau(q)}. \tag{7}$$

It can be shown[8] that $\tau(q)$ is related to the exponent $h(q)$ defined in Eq.(5) as follows:

$$\tau(q) = qh(q) - 1. \tag{8}$$

IV. THE WAVELET TRANSFORM

In this transform, the wavelet, which can be almost any chosen function, can be shifted and dilated to analyze

TABLE II: The cumulants σ^2/μ^2 , γ_1 and β_2 for the series of the high- and the low-level states' durations.

Signal	$(\sigma^2/\mu^2)_{high}$	γ_1^{high}	β_2^{high}	$(\sigma^2/\mu^2)_{low}$	γ_1^{low}	β_2^{low}
K1	1.642^a±0.008	1.963±0.009	6.75±0.04	27^a± 5	13.0^a±1.1	193^a±26
K2	1.137±0.007	1.669±0.021	5.88±0.08	2.68^a±0.25	3.22^a±0.27	15.2^b±1.9
A	0.46^a±0.09	0.8^b±0.4	3.2± 1.3	4.6^a±1.1	2.9^b±0.4	11.9±2.4
U	1.28±0.14	2.88^b±0.27	12.7± 1.7	14.3^a±0.6	7.36^a±0.28	61^a±5
n1	2.04^a±0.14	3.8±1.5	8.60±0.10	14.10^a±0.18	6.33^a±0.06	47^a±0.8
n2	2.81^a±0.12	3.38^a±0.05	16.5^a±0.4	28.1^a±1.2	11.90^a±0.24	171^a±7
n3	3.0^a±0.7	3.57^a±0.29	17.4^a±2.1	29.5^a±1.5	9.7^a± 0.3	108^a±7
n4	4.4^a±0.9	5.3^a±0.4	36^a±5	33^a±6	9.3^a±0.7	102^a±14
n5	2.8^a±0.5	2.8^b±0.4	11.6±2.5	5.7^a±0.7	5.9^a±0.4	46^a±6
n6	0.148^a±0.022	-0.23^a±0.09	2.89±0.06	0.39^a±0.04	1.74±0.08	7.09±0.20

[a] Outside the 95% confidence interval for exponentially distributed samples with the same mean and number of events.
[b] Outside the 90% confidence interval for exponentially distributed samples with the same mean and number of events.

signals(e.g., see Ref.[9]). Two variables appear in the transform: the location and the scale of the wavelet. If the wavelet ψ is translated to a point n and dilated by a factor l, then we calculate the inner product of the signal f with the function. If f shows a big change in a neighborhood of the point n it has a high-frequency spectrum there. The continuous wavelet transform of a given function $f(t)$ is defined (e.g., see Ref. [10] and references therein) with a family of test functions $\psi_{n,l}(t)$, i.e.,

$$T_\psi[f](n,l) = \langle f, \psi_{n,l} \rangle. \tag{9}$$

Each test function $\psi_{n,l}(t)$ is obtained from a *single* function $\psi(t)$ (termed analyzing wavelet) by means of a translation and a dilation $\psi_{n,l}(t) = \psi[(t-n)/l]$. where $n \in R$ and $l \in R^{++}$. $\psi(t)$ is chosen such that both its spread in time and frequency are relatively limited.

In the study of the scaling processes the following two features of the wavelet transform play key roles(e.g. Ref. [11] and references therein): (a) The wavelet basis is constructed from the dilation (change of scale) operator; thus the analyzing family exhibits a scale invariant feature. (b) $\psi(t)$ is chosen so that to have a number $n_\psi \geq 1$ of *vanishing moments*. The Fourier transform $\Psi(\omega)$ of $\psi(t)$ satisfies $|\Psi(\omega)| \sim \omega^{n_\psi}, \omega \to 0$.

A common way to build admissible wavelets of arbitrary order n_ψ is to successively differentiate a smoothing function, e.g., the Gaussian function

$$g_{n_\psi}(t) = \frac{d^{n_\psi}}{dt^{n_\psi}} e^{-t^2/2} \tag{10}$$

A. The Orthogonal Wavelet Transform

One can show that if ψ is properly chosen, then the family $\left\{2^{j/2}\psi_{j,k}\right\}_{j,k\in Z}$, with $\psi_{j,k}(t) \equiv 2^{-j}\psi(2^{-j}t - k)$ with $l_j = 2^j$ is an orthogonal basis of L^2 (e.g. see Ref.[9]). The orthogonal wavelet coefficients can then be defined by $d_f(j,k) = \langle f, \psi_{j,k} \rangle$.

Orthogonal wavelets that are often used in practice are the Daubechies wavelets, indexed by a parameter $n_D = 1, 2, \ldots$, which corresponds to the order of the wavelet. The Daubechies wavelet with $n_D = 1$ is in fact the Haar wavelet (which is discontinuous; it equals 1 at $0 \leq t < 1/2$, -1 at $1/2 < t \leq 1$ and 0 otherwise), but the Daubechies wavelets with $n_D > 1$ are continuous with bounded support, and have n_D vanishing moments.

B. The Wavelet Transform Modulus Maxima (WTMM) method

This method (e.g., see Ref. 19 of the main text and references therein) is based on the local maxima of the modulus of the continuous wavelet transform, i.e., on the local maxima n_i(over n) of the function $|T_\psi[f](n,l)|$, where l is a fixed scale. In other words, in practice, instead of averaging over all values of $|T_\psi[f](n,l)|$, one averages (within the WTMM) only the local maxima of $|T_\psi[f](n,l)|$. One sums up the $q-$th power of these maxima,

$$Z(q,l) = \sum_{i=1}^{i_{max}} |T_\psi[f](n_i,l)|^q. \tag{11}$$

If scaling behavior is observed, scaling exponents $\tau(q)$ can be defined that describe how $Z(q,l)$ scales with l:

$$Z(q,l) \sim l^{\tau(q)} \tag{12}$$

These $\tau(q)$-exponents are identical[8] to the $\tau(q)$ in Eq.(7) and related to $h(q)$ in Eq.(8). In Fig.6 of the main text, we presented the generalized Hurst exponents $h(q) = [\tau(q) + 1]/q$, where $\tau(q)$ were determined by Eq.(12) in the region of small scales l, where $\log[Z(q,l)]$ versus $\log l$ is a straight line. Note that usually in

WTMM the time-series are analyzed directly instead of the profile $y(i)$ defined in Section III.

V. METHODS IN THE "NATURAL" TIME DOMAIN

The analysis in the "natural" time-domain[12, 13] could be summarized as follows: Considering the evolution (χ_k, Q_k), the continuous function $\Phi(\omega)$ can be defined

$$\Phi(\omega) = \frac{\sum_{k=1}^{N} Q_k \exp\left(i\omega\frac{k}{N}\right)}{\sum_{k=1}^{N} Q_k} = \sum_{k=1}^{N} p_k \exp\left(i\omega\frac{k}{N}\right)$$

where $\omega = 2\pi\phi$, and ϕ stands for the *natural frequency* and $p_k = Q_k / \sum_{n=1}^{N} Q_n$. The normalized power spectrum is then defined as $\Pi(\omega) = |\Phi(\omega)|^2$. For natural frequencies ϕ less than 0.5, $\Pi(\omega)$ or $\Pi(\phi)$ reduces to a characteristic function for the probability distribution p_k in the context of probability theory. Figure 2 of the main text shows how the electric signals, mentioned in Fig.1 of the main text, are read in "natural" time, i.e., p_k or $p(\chi)$ versus χ_k or χ, respectively. Recall that[12, 13] for natural frequencies ϕ close to zero, $\Pi(\omega) = 1 - \kappa_1\omega^2 + \ldots$, with $\kappa_1 = \langle\chi^2\rangle - \langle\chi\rangle^2$, where $\langle\chi^m\rangle = \sum_k \chi_k^m p_k$ is the $m-$th "natural" moment.

A. Results of DFA

The DFA analyses for the series of the high level states' durations (see Table III of Ref.[14]) led to α_{high}-values which are close to unity for the SES activities and $\alpha_{high} \approx 0.65 - 0.8$ for the "artificial" noises. These, in reality, are the exponents that are found when DFA is applied to the "natural" time domain, i.e.,to the signals depicted in Fig.2 of the main text. This difference in the $\alpha_{high}-$ values may allow a distinction between these two types of signals. Furthermore, since $\alpha_{high} > 0.5$ for both types of signals, this excludes the possibility that the high-level states could be characterized as "random" spikes (superposed on a background level -i.e. the low state- with long range correlations, see [15]). Last but not least, we emphasize that the DFA analysis of a dichotomous Markovian process in the "natural" time domain, leads to a DFA exponent 0.5, see Fig.5(b) of the main text. In other words, since both SES activities and artificial noises lead to $\alpha > 0.5$, when analyzing them in the natural time domain, this reveals that they are both *non-Markovian* (cf. this conclusion was also obtained in Section III of the main text but on different grounds).

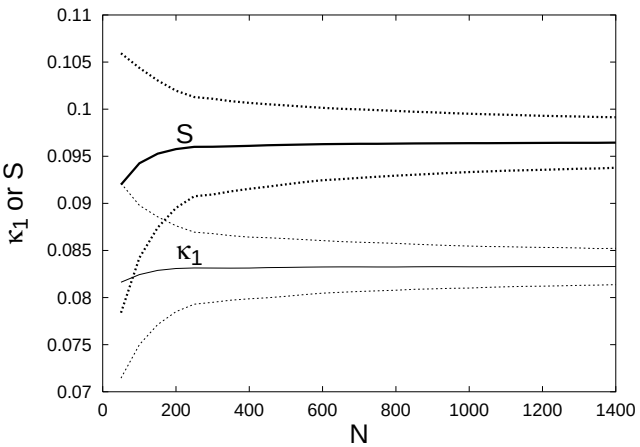

FIG. 1: Confidence intervals ($\mu \pm \sigma$) for the variance κ_1($=\langle\chi^2\rangle - \langle\chi\rangle^2$) (thin continuous lines) and the "entropy" S (thick continuous lines) calculated for a "uniform" distribution versus the number of events $N(= N_h)$(exponentially distributed data were used).

B. The "entropy" S_u and the variance κ_1 of the "uniform" distribution

As discussed in the main text the "entropy" S_u of the "uniform" distribution has the value $S_u \approx 0.0967$. Figure 1 depicts the expected value for κ_1 and S for a "uniform" distribution as a function of the number of the high level states N_h, along with their uncertainty of two standard deviations. The values of κ_1 and S for all the SES activities and "artificial" noises mentioned in Fig.1 of the main text, are shown in Table I of the main text. The fact that only n5 among the "artificial" noises seems to have a smaller "entropy" than S_u (S[n5] $= 0.091 \pm 0.011$) might be understood in the following context: For n5, we have $N_h \approx 400$ (see Table I) for which Fig.1 reveals that the aforementioned value of 0.091 differs from S_u only by an amount smaller than one standard deviation.

VI. DETRENDED FLUCTUATION ANALYSIS OF A DICHOTOMOUS SIGNAL. THE MARKOV CASE

Following Ref.[4], in the case of a Markovian dichotomous ($M = 2, m = 1, 2$) time-series the probability densities for the time spent in a single sojourn in the states "high"($m = 1$) and "low"($m = 2$) respectively, are both exponential, i.e., $p_1(T) \propto \exp(-T/\tau_{high}), p_2(T) \propto \exp(-T/\tau_{low})$ leading to the following expressions for the field-field conditional probabilities

$$P(1, t+\tau|1, t) = \tau_{eff}[\frac{1}{\tau_{low}} + \frac{\exp(-\tau/\tau_{eff})}{\tau_{high}}] \qquad (13)$$

and

$$P(2, t+\tau|1, t) = \frac{\tau_{eff}}{\tau_{high}}[1 - \exp(-\tau/\tau_{eff})], \qquad (14)$$

where $1/\tau_{eff} \equiv 1/\tau_{high} + 1/\tau_{low}$ and τ is a time lag. Note that the expressions of Eqs.(13) and (14) for the conditional probabilities satisfy the SCK equation. Moreover, the probability to observe the "high" state P_1 is

$$P_1 = \frac{\tau_{high}}{\tau_{low} + \tau_{high}}, \tag{15}$$

and the joint probability $P_{11}(\tau)$ to observe the "high" state at both the times t and $t+\tau$ is

$$P_{11}(\tau) = P_1 P(1, t+\tau | 1, t) \tag{16}$$

by the definition of the conditional probability.

The power spectral density $S(\omega)$ is the Fourier transform of the autocovariance $C(\tau) = \langle [x(t+\tau) - \langle x \rangle][x(t) - \langle x \rangle] \rangle$ of the stationary signal $x(t)$[16]:

$$C(\tau) = \langle x(t+\tau)x(t) \rangle - \langle x \rangle^2 = \frac{1}{2\pi} \int_0^\infty S(\omega) \cos(\omega\tau) d\omega. \tag{17}$$

If we assume that the states "low" and "high" have amplitudes 0 and ΔE, respectively, we have $\langle x \rangle = (\Delta E) P_1$, and $\langle x(t+\tau)x(t) \rangle = (\Delta E)^2 P_{11}(\tau)$, and, using the expressions of Eqs.(13),(15)-(17), we obtain

$$C(\tau) = (\Delta E)^2 \frac{\tau_{eff}}{\tau_{low} + \tau_{high}} \exp(-\frac{\tau}{\tau_{eff}}) \tag{18}$$

Equation (18), using the Wiener-Khinchin theorem, leads to the power spectral density

$$S(\omega) = 4 \int_0^\infty C(\tau) \cos(\omega\tau) d\tau = \frac{4(\Delta E)^2 \tau_{eff}^2}{(\tau_{low} + \tau_{high})(1 + \omega^2 \tau_{eff}^2)} \tag{19}$$

The squared variability of DFA is given, in terms of $S(\omega)$, by[16]:

$$F_{DFA}^2(l) = \frac{l}{2\pi} \int_0^\infty S(w/l) r_{DFA}(w) dw \tag{20}$$

where w denotes the *dimensionless* frequency and $r_{DFA}(w)$ is given from[16]:

$$r_{DFA}(w) = [\ w^4 \ -8w^2 - 24 - 4w^2 \cos(w) + 24\cos(w) + 24w \sin(w)]/w^6. \tag{21}$$

In Fig.4(a) of the main text, the $F_{DFA}(l)$ versus l/τ_{eff} of a dichotomous Markovian process was drawn using Eqs.(19)-(21), while Fig.4(b) of the main text depicts $S(\omega)$ versus ω/ω_{eff} where $\omega_{eff} \equiv 2\pi/\tau_{eff}$, using Eq.(19). An inspection of these figures shows that:

Concerning the power spectrum exponent β: it approaches the values 2 and 0 for the aforementioned short- and large-time scales, respectively. For time scales comparable to τ_{eff}, values of β around unity or larger(e.g. $\beta = 1.4$) can fit the data. Note that, for a given (high) frequency range, upon increasing $1/\tau_{eff}$ the calculated value of β becomes larger.

Concerning the DFA exponent α: As an example, three Markovian dichotomous time-series were constructed with $\tau_{low}/2 = \tau_{high}/2 = \tau_{eff} = 4$, 10 and 100s, and the values of $F_{DFA}(\Delta t)$ are shown in Fig.5(a) of the main text. These values are in agreement with the continuous lines that were drawn in each case using Eqs.(19)-(21). The results show the following feature: At small lags, exponents in the range $\alpha = 1.3 - 1.4 \neq 1.5$ are estimated (note that upon decreasing τ_{eff}, the $\Delta t-$range described by the exponent indicated becomes smaller). The fact that the DFA exponent approaches the value 1.5 at small lags is in quantitative agreement with the high frequency behavior of the spectrum of Eq. (19)(recall that $\alpha = 1.5$ corresponds to the case of the Brownian motion).

VII. K-MEANS CLUSTERING ALGORITHM

The K-means problem consists of dividing a set of multivariate data into non-overlapping groups in such a way as to minimize the sum (across the groups) of the sums of squared residual distances to the group centroids (this statistic is usually called Sum of Squared Errors, SSE). In other words, a computer program tries to minimize the sum, over all groups, of the squared within-groups residuals, which are the distances of the objects to the respective group centroids. The groups obtained are such that they are geometrically as compact as possible around their respective centroids. Hundreds of algorithms have been proposed to solve the K-means problem, but no algorithm can quarantee that it will find the optimum partition every time[17]. A large number of criteria have been proposed to decide on the correct number of groups in cluster analysis. Milligan and Cooper[18], after comparing 30 of these criteria, concluded that the best criterion is the one suggested by Calinski and Harabasz[19] (hereafter called C-H criterion). This is simply the F-statistic of multivariate analysis of variance and canonical analysis, where F denotes the ratio of the mean squares for the given partition divided by the mean squares for the residuals. In other words, C-H is ratio of the inter-group variance divided by the intra-group one. The best number of groups, K, present in a data set is decided upon determining the number of classes for which C-H is maximum. Here we used the K-means partitioning program provided by Ref.[20]. This program allows users to search through different values of K in a cascade, starting with k1 groups and ending with k2 groups, with k1>k2. In the cascade from a larger to the next smaller number of groups, the two groups whose centroids are the closest in multivariate space are fused and the algorithm iterates again to optimize the SSE function, reallocating objects to the groups. The whole classification process is repeated a number of times using different random starting configurations (i.e., different initial assignments of objects to the groups). The program retains the solution for each number of groups K where C-H is the highest. We run the program by considering 10 "objects", i.e., the four SES activities and the six "artificial"

noises, and using the $h(2)-$(resulting from MF-DFA in the "natural" time domain) and κ_1-values reported in Table I of the main text. Since, the physical variables are not dimensionally homogeneous, the ranging transformation: $y' = [y(i,j)-y_{min}]/(y_{max}-y_{min})$ was applied, after considering that ranging transformation is far superior to standardization (z-score transformation)[18]. A comparison of partitions from k1=5 to k2=2 groups, results in the clustering shown in Fig. 9 of the main text with the thick straight lines. This clustering corresponds to the partition for which C-H is maximum and consists of the following two groups, K=2: the first one includes the four SES activities, while the second the six "artificial" noises n1 to n6. The centroid (solid dot) of the first group (SES) lies at $\Delta\kappa = 0.013, h(2) = 0.9375$, while the centroid of the second (AN group) at $\Delta\kappa = -0.013, h(2) = 0.745$. Note that the $\Delta\kappa-$value(=1/12-κ_1) of the centroid of the group of the four SES activities corresponds to κ_1=0.070, which coincides with the theoretical value obtained from the model of critical phenomena explained in Refs.[12] and [13]. As for the two points of ICFMC, we note that they lie in the border between the aforementioned two groups. It should be noticed that when the "entropy" values (column S in Table I of the main text) are used, instead of κ_1, a comparison of partitions from k1=4 to k2=2 groups, also leads to the clustering shown in Fig. 9 of the main text.

[1] A. Fuliński, Z. Grzywna, I. Mellor, Z. Siwy, and P. N. R. Usherwood, Phys. Rev. E **58**, 919 (1998).

[2] Z. Siwy and A. Fuliński, Phys. Rev. Lett. **89**, 158101 (2002).

[3] M. Abramowitz and I. Stegun, *Handbook of Mathematical Functions* (Dover, New York, 1970).

[4] A. M. Berezhkovskii and G. H. Weiss, Physica A **303**, 1 (2002).

[5] C.-K. Peng, S. V. Buldyrev, S. Havlin, M. Simons, H. E. Stanley, and A. L. Goldberger, Phys. Rev. E **49**, 1685 (1994).

[6] S. V. Buldyrev, A. L. Goldberger, S. Havlin, R. N. Mantegna, M. E. Matsa, C.-K. Peng, M. Simons, and H. E. Stanley, Phys. Rev. E **51**, 5084 (1995).

[7] R. Weber and P. Talkner, J. Geophys. Res.-Atmos. **106**, 20131 (2001).

[8] J. Kantelhardt, S. A. Zschiegner, E. Koscielny-Bunde, A. Bunde, S. Havlin, and H. E. Stanley, Physica A **316**, 87 (2002).

[9] A. K. Louis, P. Maas, and A. Rieder, *Wavelets: Theory and Applications* (Wiley, New York, 1997).

[10] B. Audit, E. Bacry, J. Muzy, and A. Arneodo, IEEE Trans. Inf. Theory **48**, 2938 (2002).

[11] P. Abry, P. Flandrin, M. S. Taqqu, and D. Veitch, in *Self Similar Network Traffic Analysis and Performance Evaluation*, edited by K. Park and W. Willinger (Wiley, New York, 2000).

[12] P. Varotsos, N. Sarlis, and E. Skordas, Practica of the Athens Academy **76**, 388 (2001).

[13] P. A. Varotsos, N. V. Sarlis, and E. S. Skordas, Phys. Rev. E **66**, 011902 (2002).

[14] P. A. Varotsos, N. V. Sarlis, and E. S. Skordas, Phys. Rev. E **67**, 021109 (2003).

[15] Z. Chen, P. C. Ivanov, K. Hu, and H. E. Stanley, Phys. Rev. E **65**, 041107 (2002).

[16] P. Talkner and R. O. Weber, Phys. Rev. E **62**, 150 (2000).

[17] P. Legendre, K.-E. Ellingsen, E. Bjornbom, and P. Casgrain, Can. J. Fish. Aquat. Sci. **59**, 1085 (2002).

[18] G. Milligan and M. Cooper, PSYCHOMETRIKA 50 (2): 159-179 1985 **50**, 159 (1985).

[19] T. Calinski and J. Harabasz, Commun. Stat. **3**, 1 (1974).

[20] P. Legendre, Computer code K-Means available from URL `http://www.fas.umontreal.ca/BIOL/legendre` (2002).